18th Australasian Fluid Mechanics Conference
Launceston, Australia
3-7 December 2012

A numerical solution of Lighthill's acoustic analogy for acoustically excited laminar premixed flames

Mohsen Talei[1], Michael J. Brear[2] and Evatt R. Hawkes[1,3]

[1]School of Mechanical and Manufacturing Engineering
University of New South Wales, NSW 2052, Australia

[2]Department of Mechanical Engineering
University of Melbourne, VIC 3010, Australia

[3]School of Photovoltaic and Renewable Energy Engineering
University of New South Wales, NSW 2052, Australia

Abstract

This paper presents a numerical and theoretical investigation of sound generation by two-dimensional (2D) low Mach number, premixed flames. Direct Numerical Simulation (DNS) is first used to study these flames, which are excited by velocity perturbations at the inflow boundary over a range of forcing frequencies. The computational domain is fully resolved to the far-field in all cases, allowing examination of the sound radiated and its sources. Lighthill's acoustic analogy is then solved numerically using Green's functions. The radiated sound calculated using Lighthill's equation is in good agreement with that from the DNS for all cases, validating the numerical solution of Lighthill's equation. It is shown that the term involving fluctuations in the heat-release rate is not the only significant source term, contrary to the prevailing view in the literature.

Introduction

Sound generation by combusting jet flows has been the subject of considerable research, particularly over the last sixty years. Reducing noise from devices such as aircraft engines, industrial burners and diesel engines has motivated many researchers to study noise generation by different types of combusting flows. Combustion-generated sound has additional importance since its interaction with the flame may lead to thermo-acoustic instability, for example in rockets or gas-turbines [e.g. 9, 2]. To reduce the noise in such devices, the mechanisms of sound generation by reacting jet flows should be understood.

So-called 'acoustic analogies' can be used to obtain the far-field radiated sound by jet flows and investigate the sound-generation mechanisms. Acoustic analogies are a rearrangement of the equations of fluid motion into various inhomogeneous wave equations. Lighthill [10] proposed the first and best known acoustic analogy by rearranging the continuity and momentum equations only. Since then, Lighthill's equation has been used widely to investigate the mechanism of sound generation by different jet flows [e.g. 3, 2].

Strahle's work [13] appears to be the first to use an acoustic analogy to estimate the radiated sound for combusting flows. Strahle [13] argued that part of Lighthill's stress tensor featuring the density fluctuations is the dominant source term of Lighthill's equation. In his subsequent work [14], he reformulated this source term as a function of heat-release rate fluctuations and argued that the far-field sound can be estimated regardless of the turbulence structure and flame type. This result is consistent with the experimental and theoretical study by Hurle *et al.* [7] and other earlier works, but provided a more fundamental explanation as to why sound generation by flames is commonly monopolar. Indeed, variations in the heat-release rate are now commonly considered to have a significant effect on sound generation [e.g. 5, 15].

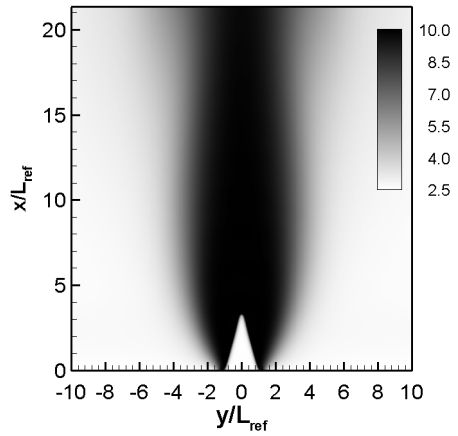

Figure 1: Steady temperature field $Tc_p/{c_u}^2$.

Direct Numerical Simulation (DNS) [e.g. 18] and Large Eddy Simulation (LES) [e.g. 8] have been used to study sound generation by reacting flows. LES has perhaps received more attention since it is computationally less expensive and is also suitable for higher Reynolds numbers. On the other hand, since all relevant features of the flame and flow are directly resolved and source terms can be directly calculated, DNS offers a unique opportunity for detailed investigations of sound generation. Nonetheless, validated solution of any acoustic analogy on an aeroacoustic DNS of a combusting jet flow, and then examining the different source terms does not appear to have been reported in the literature. This is one focus of the present paper.

The present study has two parts. First, acoustically excited premixed flame simulations that resolve both the jet flow and the acoustics will be examined. A numerical solution of Lighthill's equation then enables comparison of the source terms of Dowling's reformulation of Lighthill's equation [5] over a range of forcing frequencies.

As shown in Figure 1, the test case considered in this paper is a premixed laminar flame, surrounded by a far-field with the same temperature as the unburnt mixture. In Figure 1, T is the temperature, c_p is the specific heat constant and c is the speed of sound. The subscript u refers to the unburnt state of the mixture.

Numerical methods and flow parameters

The DNS results in this paper used a modified form of the code NTmix which features a 6^{th} order compact scheme for spatial

derivatives, combined with a 3^{rd} order Runge-Kutta time integrator [4]. NTmix has been used extensively to study combusting flows [e.g. 12, 15, 16, 1, 17]. The governing equations were discretised into 1021 streamwise nodes from $x = 0$ to $32L_{ref}$ and 541 transverse nodes from $y = 0$ to $40L_{ref}$, where L_{ref} is the half width of the flame. A non-uniform grid in both directions was set up such that the flame structure could be captured without compromising the far-field behaviour. In these simulations, the acoustic Reynolds number was $Re = \rho_u c_u L_{ref}/\mu_{ref} = 2000$ where ρ is the density and μ is the viscosity. The Prandtl number was 0.75 and the Lewis number was unity. The non-dimensionalisation Damköhler number was 129.616 and the non-dimensional laminar flame speed (*i.e.* the flame Mach number) was 0.01. The ratio of the burnt gas temperature to the fresh gas temperature was 4 and the Zel'dovich number was 8. The acoustic Mach number of the unburnt mixture jet issuing into the domain was $M_a = u_{in}/c_u = 0.04$, where u_{in} is the mean unburnt mixture velocity at the inlet on the centreline.

The velocity, temperature and mass fraction were imposed at the inflow boundary using *tanh* profiles. The inflow velocity was varied over a range of forcing frequencies at 25% of the mean inflow velocity, with the forcing frequency represented as a Strouhal number,

$$St = fL_{ref}/c_u, \tag{1}$$

where f is the frequency of excitation. The Strouhal numbers of $0.02, 0.025, 0.05, 0.1$ and 1 were used in these simulations. A symmetry boundary condition was used to simulate half of the domain. The outflow boundaries were modelled with non-reflecting boundary conditions [11].

Solution of Lighthill's acoustic analogy

Lighthill's equation in pressure form is used to study the sound generation,

$$\frac{1}{c_\infty^2}\frac{\partial^2 p}{\partial t^2} - \nabla^2 p = \frac{\partial}{\partial x_i \partial x_j}(\rho u_i u_j - \tau_{ij}) - \frac{\partial^2 \rho_e}{\partial t^2}, \tag{2}$$

where variables in the far field are denoted by a subscript ∞. In the above, p is the pressure, u is the velocity, τ is the viscous stress tensor and t is the time. The excess density is denoted:

$$\rho_e = \rho - \rho_\infty - (p - p_\infty)/c_\infty^2. \tag{3}$$

By taking the Fourier transform of equation 2, Lighthill's acoustic analogy can be expressed as a Helmholtz equation,

$$(\omega^2/c_\infty^2 + \nabla^2)\hat{p} = -\frac{\partial}{\partial x_i \partial x_j}(\widehat{\rho u_i u_j} - \widehat{\tau_{ij}}) - \omega^2 \hat{\rho}_e, \tag{4}$$

where $\hat{(\,)}$ denotes the Fourier transform of $(\,)$ and $\omega = 2\pi f$.

The solution of equation 4 for an unbounded domain can be found using free space Green's functions. However, close agreement with such a solution is not possible in the present study. This paper therefore takes an alternative approach, by developing a solution of equation 4 for a bounded domain. This solution is inevitably more complex than its free space equivalent. However, it can be validated against the numerical simulations, thus giving confidence in subsequent analysis of individual acoustic source terms. It also permits separation of the sound generated by the flow itself from that radiated by the inflow excitation.

This bounded domain Green's function solution of equation 4 can be expressed as,

$$\hat{p}(\mathbf{r_0},\omega) = \int_{A_0} f(\mathbf{r}) G(\mathbf{r}|\mathbf{r_0}) dA - \int_{l_0} \hat{p}(\mathbf{r},\omega) \nabla G(\mathbf{r}|\mathbf{r_0}).\mathbf{n} dl + \int_{l_0} G(\mathbf{r}|\mathbf{r_0}) \nabla \hat{p}(\mathbf{r},\omega).\mathbf{n} dl, \tag{5}$$

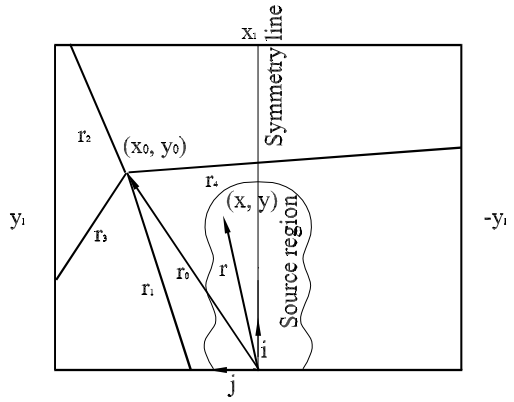

Figure 2: Schematic of the coordinate system and the source region.

where

$$f(\mathbf{r}) = \frac{\partial}{\partial x_i \partial x_j}(\widehat{\rho u_i u_j} - \widehat{\tau_{ij}}) + \omega^2 \hat{\rho}_e, \tag{6}$$

and G is the Green's function. The terms A_0 and l_0 are the area and boundary of the source region. If the boundaries have no reflections or acoustic energy flux, the corresponding integral terms will be zero. However, when the flow is excited at the inflow or the boundary passes through the source region, these terms are non-zero and must be retained.

The Green's function for a 2D problem can be expressed using a Hankel function,

$$G(\mathbf{r}|\mathbf{r_0}) = \frac{i}{4} H_0^{(1)}(\kappa|\mathbf{r} - \mathbf{r_0}|), \tag{7}$$

where

$$\kappa = \omega/c_\infty. \tag{8}$$

Using equation 7 for the 2D problem shown in Figure 2 and the method of images [6] the resulting Fourier transform of the pressure can be considered as a sum of the components,

$$\hat{p} = \hat{p}_{in} + \hat{p}_{st} + \hat{p}_{ex}, \tag{9}$$

where

$$\hat{p}_{in}(\mathbf{r_0},\omega) = \frac{i}{4}\int_{A_0} f(\mathbf{r}) H_0^{(1)}(\kappa|\mathbf{r}' - \mathbf{r_0}|) dA + \frac{i}{4}\int_{-y_l}^{y_l} \frac{\partial \hat{p}}{\partial x}(\mathbf{r},\omega)\bigg|_{x=0} H_0^{(1)}(\kappa r_1) dy, \tag{10}$$

$$\hat{p}_{st}(\mathbf{r_0},\omega) = \frac{i}{4}\int_{A_0} \frac{\partial(\widehat{\rho u_i u_j} - \widehat{\tau_{ij}})}{\partial x_i \partial x_j} H_0^{(1)}(\kappa|\mathbf{r} - \mathbf{r_0}|) dA, \quad \text{and} \tag{11}$$

$$\hat{p}_{ex}(\mathbf{r_0},\omega) = \frac{i\omega^2}{4}\int_{A_0} \hat{\rho}_e H_0^{(1)}(\kappa|\mathbf{r} - \mathbf{r_0}|) dA. \tag{12}$$

The variables $\hat{p}_{in}$, $\hat{p}_{st}$ and $\hat{p}_{ex}$ describe the respective contribution of the inflow boundary, the part of Lighthill's stress tensor including the Reynolds-stress term and the excess density term to the radiated sound.

The variable $\hat{p}_{ex}$ in equation 12 can be reformulated using Dowling's reformulation [5] of Lighthill's equation as follows,

$$\hat{p}_{ex} = \hat{p}_{hr} + \hat{p}_{th} + \hat{p}_{vis} + \hat{p}_{ex1} + \hat{p}_{ex2}, \tag{13}$$

where

$$\hat{p}_{hr}(\mathbf{r_0},\omega) = \frac{i\omega\rho_\infty Q}{4}\int_{A_0} \left(\widehat{\frac{\dot{\omega}}{\rho c_p T}}\right) H_0^{(1)}(\kappa|\mathbf{r} - \mathbf{r_0}|) dA, \tag{14}$$

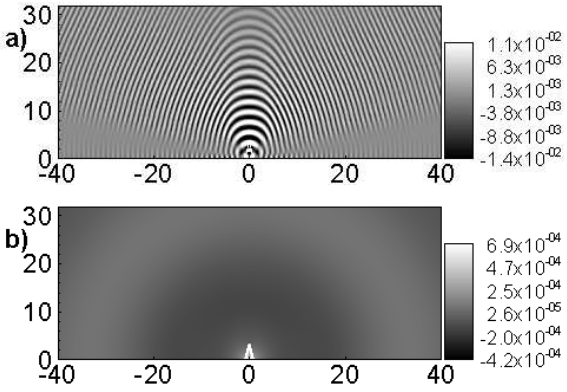

Figure 3: Instantaneous dilatation field $L_{ref}\nabla.u/c_u$ for a) $St = 1$ and b) $St = 0.05$.

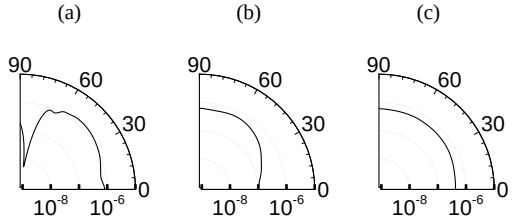

Figure 4: Non-dimensional RMS pressure ${p_{rms}}^2/{\rho_u}^2{c_u}^4$ for a) $St = 1$, b) $St = 0.05$ and c) $St = 0.02$ at $20L_{ref}$ radius.

$$\hat{p}_{th}(\mathbf{r_0},\omega) = \frac{i\omega\rho_\infty}{4}\int_{A_0}\left(\widehat{\frac{\nabla.q}{\rho c_p T}}\right)H_0^{(1)}(\kappa|\mathbf{r}-\mathbf{r_0}|)dA, \quad (15)$$

$$\hat{p}_{vis}(\mathbf{r_0},\omega) = \frac{i\omega\rho_\infty}{4}\int_{A_0}\left(\widehat{\frac{\tau_{ij}\partial u_i/\partial x_j}{\rho c_p T}}\right)H_0^{(1)}(\kappa|\mathbf{r}-\mathbf{r_0}|)dA, \quad (16)$$

$$\hat{p}_{ex1}(\mathbf{r_0},\omega) = \frac{i\omega}{4c_\infty^2}\int_{A_0}\left[\left(1-\frac{\rho_\infty c_\infty^2}{\rho c^2}\right)\widehat{\frac{Dp}{Dt}} - \frac{p-p_\infty}{\rho}\frac{D\rho}{Dt}\right]H_0^{(1)}(\kappa|\mathbf{r}-\mathbf{r_0}|)dA, \quad (17)$$

and

$$\hat{p}_{ex2}(\mathbf{r_0},\omega) = \frac{i\omega}{4}\int_{A_0}\frac{\partial}{\partial x_i}\widehat{(u_i\rho_e)}H_0^{(1)}(\kappa|\mathbf{r}-\mathbf{r_0}|)dA. \quad (18)$$

In the above, Q is the specific heat of reaction, $\dot{\omega}$ is the reaction rate and q is the heat flux. The variables $\hat{p}_{hr}$, $\hat{p}_{th}$ and $\hat{p}_{vis}$ are the effects of heat release, heat conduction and viscous stress on the radiated sound, respectively. Terms $\hat{p}_{ex1}$ and $\hat{p}_{ex2}$ are due to the effects of density inhomogeneities.

Results and discussion

DNS results

Figures 3a and b show the dilatation field $\nabla.\mathbf{u}$ at an instant for $St = 1$ and 0.05. Directionality of the acoustic field is observed at the high frequency limit ($St = 1$). This can also be seen in Figure 4a. As shown in Figure 4b, monopolar behaviour is observed at low to intermediate forcing frequencies. Later analysis will show that this monopolar behaviour is due to both the contribution of the inflow boundary and monopolar source terms in Lighthill's equation.

Numerical solution of Lighthill's equation

Equation 4 was solved numerically. Figure 5 shows a comparison between this solution of Lighthill's equation and the DNS results. The DNS and solution of Lighthill's equation agree very well in all cases, validating the numerical solution. It can also be observed that the inflow boundary significantly contributes to the solution of Lighthill's equation at $St = 0.05$.

The magnitudes of $\hat{p}_{st}$ and $\hat{p}_{ex}$ defined in equations 11 and 12 evaluated at $x = 0.1L_{ref}$, $y = 30L_{ref}$ are shown in Figure 6 for all cases. As can be seen, the excess density term is the dominant source term. The magnitudes of $\hat{p}_{hr}$, $\hat{p}_{th}$, $\hat{p}_{visc}$, $\hat{p}_{ex1}$ and $\hat{p}_{ex2}$ defined in equations 14-18 are shown in Figure 7. The density inhomogeneity term $\hat{p}_{ex1}$ is small compared with the other terms for all cases. The viscous stress term $\hat{p}_{vis}$ is also negligible for all cases studied here. However, it can be observed that $\hat{p}_{ex2}$, which represents changes in the momentum of density inhomogeneities, dominates the other source terms.

Figure 7 also shows that both $\hat{p}_{hr}$ and $\hat{p}_{ex2}$ are significant source terms. The relative contribution of the heat release term $\hat{p}_{hr}$ increases as the excitation frequency decreases. However, the excess density term $\hat{p}_{ex2}$ remains the dominant term for $St > 0.05$. This contradicts the view that the heat release source term is the only significant term in this problem. The term due to heat conduction, $\hat{p}_{th}$ is comparable to $\hat{p}_{hr}$ for $St \geq 0.1$. This may be expected since heat conduction and heat release are intimately connected in premixed flames, and demonstrates once again that $\hat{p}_{hr}$ is not the only significant source term.

Conclusions

Acoustically forced laminar jet flames have been studied numerically. The sound radiated was directional at high forcing frequency, but monopolar at low forcing frequency in all cases.

Lighthill's equation as reformulated by Dowling [5] was employed to examine the relative importance of the source terms involved in these flames. Since the far field was resolved in the DNS, validation of the numerical solution of Lighthill's equation was first performed, providing a solid basis on which to discuss the relative magnitude of different source terms in Lighthill's equation.

As expected, the so-called 'excess density' term in Lighthill's equation was observed to be significantly larger than the 'Reynolds stress term' for all cases. More surprisingly, however, decomposition of this excess density term revealed that, in the limit of high forcing frequency, the term describing changes in the momentum of density inhomogeneities was the dominant source term. At intermediate frequencies, this term due to density inhomogeneities was still comparable in magnitude to the heat-release source term. It therefore appears that considering the heat release fluctuations to be the dominant source of sound for low Mach number, combusting flows is problematic.

Acknowledgements

The authors acknowledge the generous support of the Australian Research Council (ARC) and the European Centre for Research and Advanced Training in Scientific Computation (CERFACS, www.cerfacs.fr), in providing the authors with the source code for NTmix. Use of the facilities of the Victorian Partnership for Advanced Computing (VPAC) is also acknowledged.

References

[1] Brear, M. J., Nicoud, F., Talei, M., Giauque, A. and Hawkes, E. R., Disturbance energy transport and sound

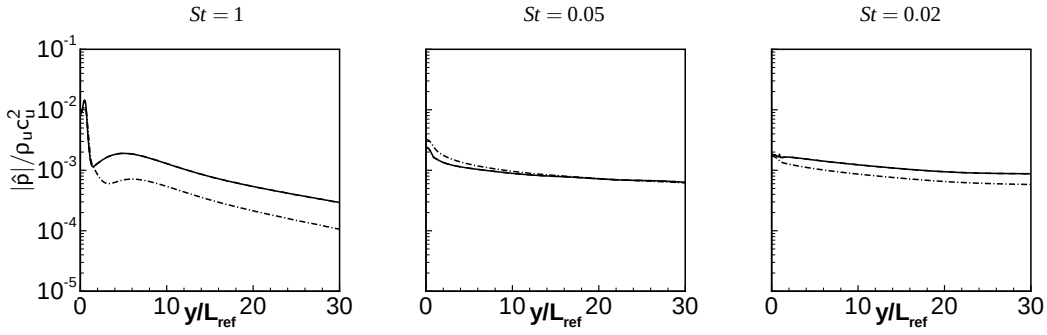

Figure 5: Comparison of complete solution of Lighthill's equation for $|\hat{p}|$ (solid line), DNS (dashed), solution of Lighthill's equation including only the inflow boundary term (dash-dot) at the angle of 90° with respect to the jet axis and near the inflow boundary. Note that the DNS line is obscured by the solution of Lighthill's equation.

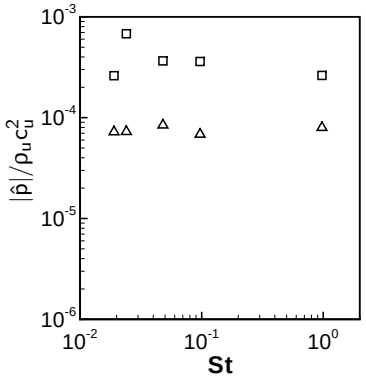

Figure 6: Magnitude of $\hat{p}_{st}$ (▵) and $\hat{p}_{ex}$ (□) versus Strouhal number.

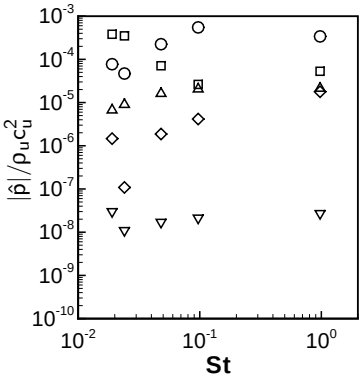

Figure 7: Magnitude of $\hat{p}_{hr}$ (□), $\hat{p}_{th}$ (▵), $\hat{p}_{vis}$ (▽), $\hat{p}_{ex1}$ (◇) and $\hat{p}_{ex2}$ (○) at $(x = 0.1L_{ref}, y = 30L_{ref})$ versus Strouhal number.

production in gaseous combustion, *J. Fluid Mech.*, **707**, 2012, 53–73.

[2] Candel, S., Durox, D., Ducruix, S., Birbaud, A. L., Noiray, N. and Schuller, T., Flame dynamics and combustion noise: progress and challenges, *Int. J. Aeroacoustics*, **8**, 2009, 1–56.

[3] Colonius, T. and Lele, S. K., Computational aeroacoustics: progress on nonlinear problems of sound generation, *Prog. Aerosp. Sci.*, **40**, 2004, 345–416.

[4] Cuenot, B., Bédet, B. and Corjon, A., *NTMIX3D user's guide manual*, 1997.

[5] Dowling, A. P., *Modern Methods in Analytical Acoustics*, Springer, 1992 378–403.

[6] Duffy, D. G., *Green's Functions with Applications*, Chapman & Hall/CRC, 2001.

[7] Hurle, I. R., Price, R. B., Sugden, T. M. and Thomas, A., Sound emission from open turbulent premixed flames, *Proc. Roy. Soc.*, **303**, 1968, 409–427.

[8] Ihme, M. and Pitsch, H., On the generation of direct combustion noise in turbulent non-premixed flames, *Int. J. Aeroacoustics*, **11**, 2012, 25–78.

[9] Lieuwen, T., Modeling premixed combustion-acoustic wave interactions: A review, *J. Propul. Power*, **19**, 2003, 765–781.

[10] Lighthill, M. J., On sound generation aerodynamically I. General theory, *Proc. Roy. Soc.*, **211**, 1951, 564–587.

[11] Lodato, G., Domingo, P. and Vervisch, L., Three-dimensional boundary conditions for direct and large-eddy simulation of compressible viscous flows, *J. Comput. Phys.*, **227**, 2008, 5105–5143.

[12] Poinsot, T. J. and Lele, S. K., Boundary conditions for direct simulations of compressible viscous flows, *J. Comput. Phys.*, **101**, 1992, 104–129.

[13] Strahle, W. C., On combustion generated noise, *J. Fluid Mech.*, **49**, 1971, 399–414.

[14] Strahle, W. C., Some results in combustion generated noise, *J. Sound Vib.*, **23**, 1972, 113–125.

[15] Talei, M., Brear, M. J. and Hawkes, E. R., Sound generation by laminar premixed flame annihilation, *J. Fluid Mech.*, **679**, 2011, 194–218.

[16] Talei, M., Brear, M. J. and Hawkes, E. R., A parametric study of sound generation by laminar premixed flame annihilation, *Combust. Flame*, **159(2)**, 2012, 757–769.

[17] Talei, M., Hawkes, E. R. and Brear, M. J., A direct numerical simulation study of frequency and Lewis number effects on sound generation by two-dimensional forced laminar premixed flames, *Proc. Combust. Inst.*, http://dx.doi.org/10.1016/j.proci.2012.07.034.

[18] Zhao, W. and Frankel, S. H., Numerical simulations of sound radiated from an axisymmetric premixed reacting jet, *Phys. Fluids*, **13**, 2001, 2671–2681.